THE JOURNAL OF BIOLOGICAL CHEMISTRY VOL. 287, NO. 45, pp. 37703–37712, November 2, 2012

The Oxidation-sensing Regulator (MosR) Is a New Redox-dependent Transcription Factor in *Mycobacterium tuberculosis*[*] [S]

Received for publication, July 5, 2012, and in revised form, September 17, 2012 Published, JBC Papers in Press, September 19, 2012, DOI 10.1074/jbc.M112.388611

Pedro Brugarolas[‡], Farahnaz Movahedzadeh[§], Yuehong Wang[§], Nan Zhang[§], Iona L. Bartek[¶], Yihe N. Gao[‡], Martin I. Voskuil[¶], Scott G. Franzblau[§], and Chuan He[‡1]

From the [‡]Department of Chemistry and Institute for Biophysical Dynamics, The University of Chicago, Chicago, Illinois 60637, the [§]Institute for Tuberculosis Research, College of Pharmacy, University of Illinois, Chicago, Illinois 60612, and the [¶]Department of Microbiology, School of Medicine, University of Colorado Denver, Aurora, Colorado 80045

Background: *Mycobacterium tuberculosis* is an intracellular pathogen that survives under oxidative stress for which none of the common bacterial oxidation sensors have been described.
Results: A new oxidation sensor of *M. tuberculosis* is described.
Conclusion: MosR is a new thiol-based oxidation-sensing regulator of the MarR family.
Significance: *M. tuberculosis* must adapt to oxidative environments; therefore, targeting MosR or MosR-regulated proteins may provide ways to fight this bacterium in the future.

Mycobacterium tuberculosis **thrives in oxidative environments such as the macrophage. To survive, the bacterium must sense and adapt to the oxidative conditions. Several antioxidant defenses including a thick cell wall, millimolar concentrations of small molecule thiols, and protective enzymes are known to help the bacterium withstand the oxidative stress. However, oxidation-sensing regulators that control these defenses have remained elusive. In this study, we report a new oxidation-sensing regulator, Rv1049 or MosR (*M. tuberculosis* oxidation-sensing regulator). MosR is a transcriptional repressor of the MarR family, which, similarly to *Bacillus subtilis* OhrR and *Staphylococcus aureus* MgrA, dissociates from DNA in the presence of oxidants, enabling transcription. MosR senses oxidation through a pair of cysteines near the N terminus (Cys-10 and Cys-12) that upon oxidation forms a disulfide bond. Disulfide formation rearranges a network of hydrogen bonds, which leads to a large conformational change of the protein and dissociation from DNA. MosR has been shown previously to play an important role in survival of the bacterium in the macrophage. In this study, we show that the main role of MosR is to up-regulate expression of *rv1050* (a putative exported oxidoreductase that has not yet been characterized) in response to oxidants and propose that it is through this role that MosR contributes to the bacterium survival in the macrophage.**

Thanks to impressive international efforts, the rate of *Mycobacterium tuberculosis* infections is beginning to decrease (1). However, with an estimated 8.8 million cases of tuberculosis and 1.1 million deaths reported in 2010, there is still plenty to do before we can foresee the possible eradication of the disease. In addition, the demographics of the disease (it mostly occurs in developing countries), the vast reservoir for potential reactivation (up to one-third of the world population is latently infected), and the emergence of drug-resistant strains (650,000 estimated prevalent cases in 2010) make accomplishing its eradication a formidable task (1). Although current therapies are effective in killing the bacterium, they require multiple months of therapy, which reduces the compliance of patients and increases the risk of drug resistance. To develop superior therapies and vaccines, we need to gain better understanding of the physiology of the bacterium.

A poorly understood aspect of *M. tuberculosis* is the exact mechanism of how it detects and evades the host immune system. To survive inside macrophages, *M. tuberculosis* must withstand reactive oxygen species (ROS)[2] produced by phagocyte oxidase (NOX2/gp91^{phox}) and reactive nitrogen species (RNS) produced by inducible nitric-oxide synthase in the macrophage (2). The bacterium is aided by several antioxidant defenses including a thick cell wall rich in lipoarabinomannan, cyclopropanated mycolic acid, and phenolic glycolipid I (PGL-1) (3), millimolar concentration of mycothiol (4, 5), protective enzymes such as catalase (KatG) (6), superoxide dismutases (SodA and SodC) (7, 8), peroxidase and peroxynitrite reductase complex (AhpC, AhpD, SucB, and Lpd) (9, 10), and DNA-binding proteins such as Lrs2 (11), as well as an arsenal of exported proteins (12). However, little is known of transcriptional regulators sensitive to oxidation in *M. tuberculosis* that control these cellular defenses.

Transcriptional regulators responsive to oxidative stress are crucial for many pathogenic bacteria (13–15). For example,

* This work was supported, in whole or in part, by National Institutes of Health Grant AI074658 (to C. H.) from the NIAID. This work was also supported by the Chicago Biomedical Consortium with support from The Searle Funds at the Chicago Community Trust (to C. H. and S. G. F.), a Burroughs Wellcome Fund Investigator in the Pathogenesis of Infectious Disease Award (to C. H.), National Institutes of Health Grant R01 AI061505 (to M. I. V.), and a Graduate Fellowship from Fundación Caja Madrid (to P. B.).
[S] This article contains supplemental Figs. S1–S7, Tables S1–S5, and Experimental Procedures.
The atomic coordinates and structure factors (codes 4FX0 and 4FX4) have been deposited in the Protein Data Bank (http://wwpdb.org/).
[1] To whom correspondence should be addressed: Dept. of Chemistry and Institute for Biophysical Dynamics, The University of Chicago, GCIS 319B, 929 E. 57th St., Chicago, IL 60637. Tel.: 773-702-5061; Fax: 773-702-0805; E-mail: chuanhe@uchicago.edu.

[2] The abbreviations used are: ROS, reactive oxygen species; RNS, reactive nitrogen species; MosR, *M. tuberculosis* oxidation-sensing regulator; Ohr, organic hydroperoxide resistance protein.

Staphylococcus aureus MgrA controls the transcriptional regulation of ~350 genes in *S. aureus* and is a major virulence factor (16–18). In *Pseudomonas aeruginosa*, OxyR and SoxR control the expression of antioxidant genes and DNA repair enzymes that confer resistance to oxidative stress, antibiotics, heavy metals, and macrophage killing (19–21). Unlike reductive stress regulators such as WhiB3, which have been well characterized in recent years (22, 23), no oxidative stress regulators homologous to SoxR, OxyR, and OhrR have been described in *M. tuberculosis* to date. OxyR, although present in related species such as *Mycobacterium leprae*, has acquired several nonsense mutations in *M. tuberculosis*, and it is nonfunctional; SoxR, also present in the related species *Mycobacterium smegmatis*, does not have a homolog in *M. tuberculosis*; and so far, no MgrA/OhrR homologs have been described in *M. tuberculosis*.

Recently, Voskuil *et al.* (24) examined the transcriptional response of *M. tuberculosis* to ROS and RNS. They found that under low concentrations of H_2O_2 (0.05 and 0.5 mM), only *furA*, the regulator of catalase peroxidase (KatG), was induced. Concentrations of 50 mM or higher were lethal to the bacteria and gave relatively few transcriptional changes. Intermediate concentrations between 5 and 10 mM caused a number of genes and regulators to be induced including those involved in iron response, iron-sulfur cluster repair, ROS/RNS damage repair, and DNA repair. They concluded that besides FurA (25), IdeR (26), SigH (27), and SigE (28), which had been previously implicated in ROS resistance, there are 14 other unstudied regulators that can be induced upon ROS. In this study, we describe a new oxidation-sensitive transcriptional regulator in *M. tuberculosis*, a homolog of *Bacillus subtilis* OhrR and *S. aureus* MgrA that we named MosR (*M. tuberculosis* oxidation-sensing regulator) and propose a molecular mechanism for MosR in the context of infection.

EXPERIMENTAL PROCEDURES

All procedures involving live *M. tuberculosis* were carried out in a biosafety level III laboratory. Additional details for these and other experimental procedures can be found in the supplemental Experimental Procedures.

Protein Expression and Purification—All the MosR protein variants were expressed in *Escherichia coli* using the codon-optimized sequence on a modified pET28a vector containing a thrombin-cleavable C-terminal His tag. After overnight expression at 16 °C, the protein was purified by nickel-nitrilotriacetic acid affinity chromatography. Plasmids and primers used for cloning and expression are shown in supplemental Tables S1 and S2.

Protein Crystallization, X-ray Data Collection, Structure Determination, and Refinement—For crystallization purposes, a construct containing a four-amino acid truncation on the N terminus (amino acids 2–5) was used. Crystallization experiments were carried out using hanging-drop vapor diffusion at room temperature and 16 °C. Datasets on frozen crystals were collected at beamline 24-ID of the Argonne National Laboratory. All data were indexed, integrated, and scaled using HKL2000 (29). The structure of MosR-DNA complex was solved by molecular replacement in Phaser (30) using a model derived from the structure of OhrR with DNA (Protein Data Bank (PDB) ID 1Z9C) (31). To solve apo-MosR, we used a model based on the newly obtained structure of MosR-DNA. The structures were refined using PHENIX (32) and Coot (33). Figures were prepared using PyMOL (34). Full data collection and refinement statistics can be found in supplemental Table S3.

Electrophoretic Mobility Shift Assays—Purified recombinant MosR (50 nM) was combined with a ^{32}P-labeled DNA (5 nM) corresponding to the 100–300-bp region upstream of the gene under investigation in the presence of excess salmon-sperm DNA and different concentration of oxidants as specified in Fig. 3. The mixture was incubated at room temperature for 30 min. DTT was added to the specified samples 15 min after the addition of the oxidant. Samples were run on 4% polyacrylamide native gels, and afterward the gels were dried and exposed to a phosphor screen overnight, and images acquired using a Bio-Rad Pharos FX molecular imager.

DNase I Footprinting Assay and Sequencing Reactions—DNase I footprinting assay was carried out using the protocol from Leblanc and Moss (35). Briefly, 50 nM DNA corresponding to the promoter region labeled on one end only was combined with 500 nM protein in the presence of 1 mM DTT. 0.5 units of DNase I were added to the mix and allowed to react for 4 min. Then the reaction was stopped by the addition of STOP solution. Sequencing reactions were performed using the Sequenase kit from Affymetrix. Both samples were run side-by-side on a 4% native gel. The images were acquired as in the electrophoretic mobility shift assays.

Construction of M. tuberculosis Mutant Strains—Δ*mosR* strain was constructed using the pGOAL/p2NIL system developed by Parish and Stoker (36). Complementation strains were prepared by transforming Δ*mosR* strain with the appropriate plasmid. A list with the plasmids used in this study can be found in supplemental Table S1.

RNA Isolation and Microarray—RNA isolation and microarray were performed as reported previously (24, 37).

RT-PCR—RT-PCR was performed using SuperScript one-step RT-PCR system (Invitrogen). Primers used are shown in supplemental Table S2.

RESULTS

MosR Is an OhrR/MgrA Homolog—Intrigued by the lack of obvious oxidation-sensing regulators in *M. tuberculosis*, we decided to look for homologs of *B. subtilis* OhrR and *S. aureus* MgrA in *M. tuberculosis H37Rv* proteome. A direct BLAST-P search for homologs yielded no hits in *M. tuberculosis*, but found one candidate in the closely related species *M. smegmatis* that belongs to the MarR family, MSMEG_0448 (43% identical over 145 amino acids to OhrR and 35% identical over 143 amino acids to MgrA). MSMEG_0448 as an OhrR homolog is further supported by the recent discovery that adjacent protein MSMEG_0447, is a homolog of organic hydroperoxide resistance protein (Ohr) (38). A subsequent search for homologs of MSMEG_0448 found one potential candidate in *M. tuberculosis*: Rv1049 (26% identical over 147 amino acids) (Fig. 1, supplemental Fig. S1) that we named MosR. Although MosR is only 28% identical over 103 amino acids to OhrR and 28% identical over 106 amino acids to MgrA, we thought it might share an

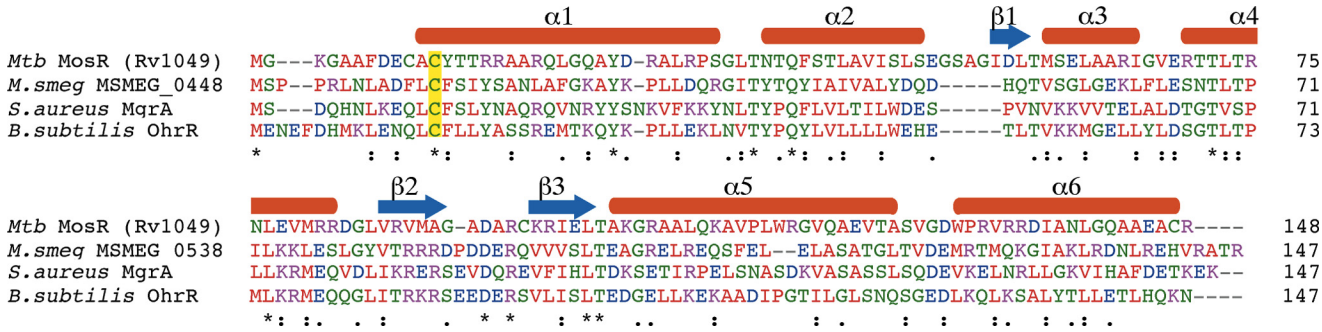

FIGURE 1. **MosR (Rv1049) is an OhrR/MgrA homolog.** ClustalW sequence alignment of *M. tuberculosis* MosR (*Mtb MosR*), *M. smegmatis* MSMEG_0448, *S. aureus* MgrA, and *B. subtilis* OhrR. Conserved Cys is highlighted in *yellow*. Amino acids are colored according to physicochemical properties. *Asterisks* indicate conserved residues; *colons* indicate highly similar residues; *periods* indicate less similar residues.

oxidation-sensing mechanism as it contains the cysteine presumed to serve for oxidation sensing in a conserved position (Cys-12) and an additional adjacent cysteine (Cys-10) not conserved in OhrR/MgrA. In addition, in these oxidation-sensing regulators, the conserved cysteine is typically surrounded by aromatic amino acids (39), which are also conserved in MosR (Tyr-13, Tyr-26, and Phe-40).

MosR Contains a Reversible Disulfide Bond between Cys-10 and Cys-12—After failed attempts to express MosR in *E. coli* from the native DNA sequence, we turned to a synthetic variant containing the codon-optimized sequence for *E. coli*. This construct expressed well, and we were able to purify the protein to reasonable yields (0.1 mg/liter) and high purity using a nickel-nitrilotriacetic acid column (Fig. 2*A*). We noticed that if the protein was purified in the absence of reducing agents, a new band with retarded mobility appeared on a nonreducing SDS-PAGE gel, suggesting partial oxidation and formation of an intramolecular disulfide bond that may induce a conformational change of the protein (Fig. 2*B*). We then sought to identify and confirm the disulfide bond using mass spectrometry.

For this experiment, we subjected MosR to three different conditions (1 mM DTT, 1 h of air oxidation, and 5 mM H_2O_2) followed by alkylation, trypsin digestion, and LC-MS/MS analysis. In the presence of 1 mM DTT, we found no evidence for the presence of disulfide bonds in the protein. Under air oxidation, which mimics the conditions in which we observe a double band on SDS-PAGE gel, we found one disulfide bond between Cys-10 and Cys-12 (Fig. 2*C*). Under 5 mM H_2O_2, we found evidence for two disulfide bonds with one between Cys-10 and Cys-12 and another between Cys-96 and Cys-147 (supplemental Fig. S2). These data show that formation of disulfide between Cys-10 and Cys-12 is more facile and likely represents the primary biological mechanism used by MosR to sense oxidation.

Reduced MosR Binds to DNA, whereas Oxidized MosR Does Not—To test whether MosR functions as an oxidation-sensing transcriptional regulator, we tested its ability to bind to DNA in the presence of oxidants. We speculated that similar to other MarR proteins, MosR would be autoregulated, and therefore we chose a 300-bp fragment of DNA directly upstream of the *mosR* gene to test for DNA binding. The protein bound to the amplified DNA even in the presence of 10-fold excess of non-specific DNA with a K_d of ~15 nM (supplemental Fig. S3*A*). Subsequently, we tested the ability of the protein to bind DNA in the presence of increasing concentrations of oxidants including H_2O_2, cumene hydroperoxide and *tert*-butyl hydroperoxide, and the NO precursor spermine-NONOate (Fig. 3, *A–C*, supplemental Fig. S3*B*). In all cases, except with the NO precursor, we saw dissociation of the protein from DNA upon the addition of 0.5–1 mM of the respective oxidant. This dissociation was reversible upon the addition of the reducing agent, DTT (Fig. 3, *A–C*). Spermine-NONOate did not cause dissociation of the protein from the DNA up to 1 mM, and concentrations of 10 mM or higher led to protein aggregation due to the tendency of spermine to precipitate proteins.

We then assayed the role of the cysteines in oxidation-dependent DNA binding. MosR contains four cysteines: Cys-10, Cys-12, Cys-96, and Cys-147. Only Cys-12 is conserved among oxidation-sensing OhrR/MgrA proteins, and thus we focused our attention on this cysteine and the proximal Cys-10. Substitution of Cys-10 or Cys-12 by serine results in proteins with lower sensitivity to oxidation as shown in Fig. 3*D*. Under the assayed conditions, treatment with 1 mM H_2O_2 for 1 h is sufficient to completely dissociate the wild-type MosR but not the Cys-to-Ser substituted proteins. Double mutation of Cys-10 and Cys-12 to serine results in a protein with decreased DNA binding affinity even under reducing conditions. In our experience, substitution of Cys to Ser in this family of proteins often affects the stability of the protein. The partial dissociation of MosR-C10S and MosR-C12S with >1 mM H_2O_2 may be due to non-specific oxidation of the protein or additional oxidation-sensing mechanisms. Nonetheless, the lower sensitivity of the substituted proteins with Cys-10 and Cys-12 replaced by Ser suggests that these residues play important roles in the oxidation-sensing mechanism, which is consistent with disulfide bond formation between these two residues. This type of behavior in which substitution from Cys-12 to Ser results in a protein less responsive to oxidation is reminiscent of OhrR and MgrA (16, 40).

MosR Binds to a Specific DNA Sequence and Controls the Expression of Redox-related Genes—We then performed a DNase I footprinting assay to determine the specific sequence that MosR binds. A 26-base-long quasi-palindromic motif starting 31 bases upstream of *mosR* (*rv1049*) starting codon was revealed as the binding site of MosR (Fig. 4*A*). A pattern search for similar sequences in the genome of *M. tuberculosis* unveiled similar sequences in the promoter regions of *rv1050*, *ndhA*, *narL*, *narX*, *ndhA*, and *esxR* (Fig. 4*B*). We then tested for bind-

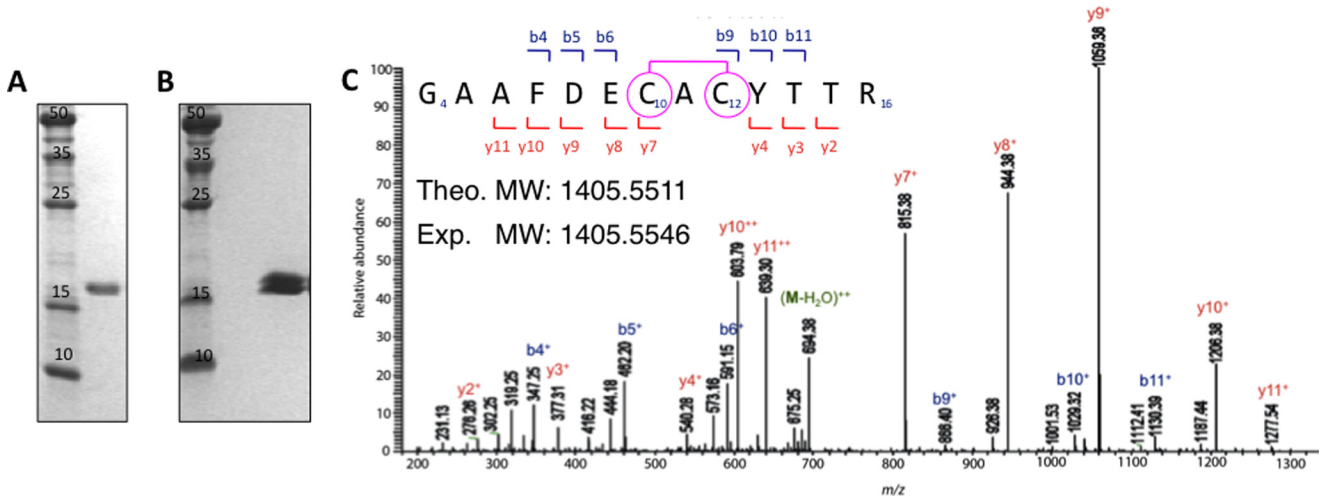

FIGURE 2. **MosR forms a reversible disulfide bond upon oxidation.** *A*, SDS-PAGE gel showing purified reduced MosR. *B*, double band on nonreducing SDS-PAGE indicates partially oxidized protein. *C*, LC-MS/MS spectrum of peptide fragment ^{4}GAAFDECACYTTR^{16} (observed *m/z* 1405.5546 corresponding to peptide theoretical mass of 1407.5321 Da minus two hydrogen atoms (−2 Da)) obtained after trypsin digestion of oxidized MosR. The fragment ions $y7^{+}$ and $b9^{+}$ corresponding to ^{4}GAAFDECAC^{12} and ^{10}CACYTTR^{16}, respectively (observed *m/z* 815.38 and 886.40) indicate the presence of disulfide bond between Cys-10 and Cys-12. Fragment ion arising from the neutral loss of water (−18 Da) is marked as *M-H_2O*. *Theo. MW*, theoretical molecular weight; *Exp. MW*, experimental molecular weight.

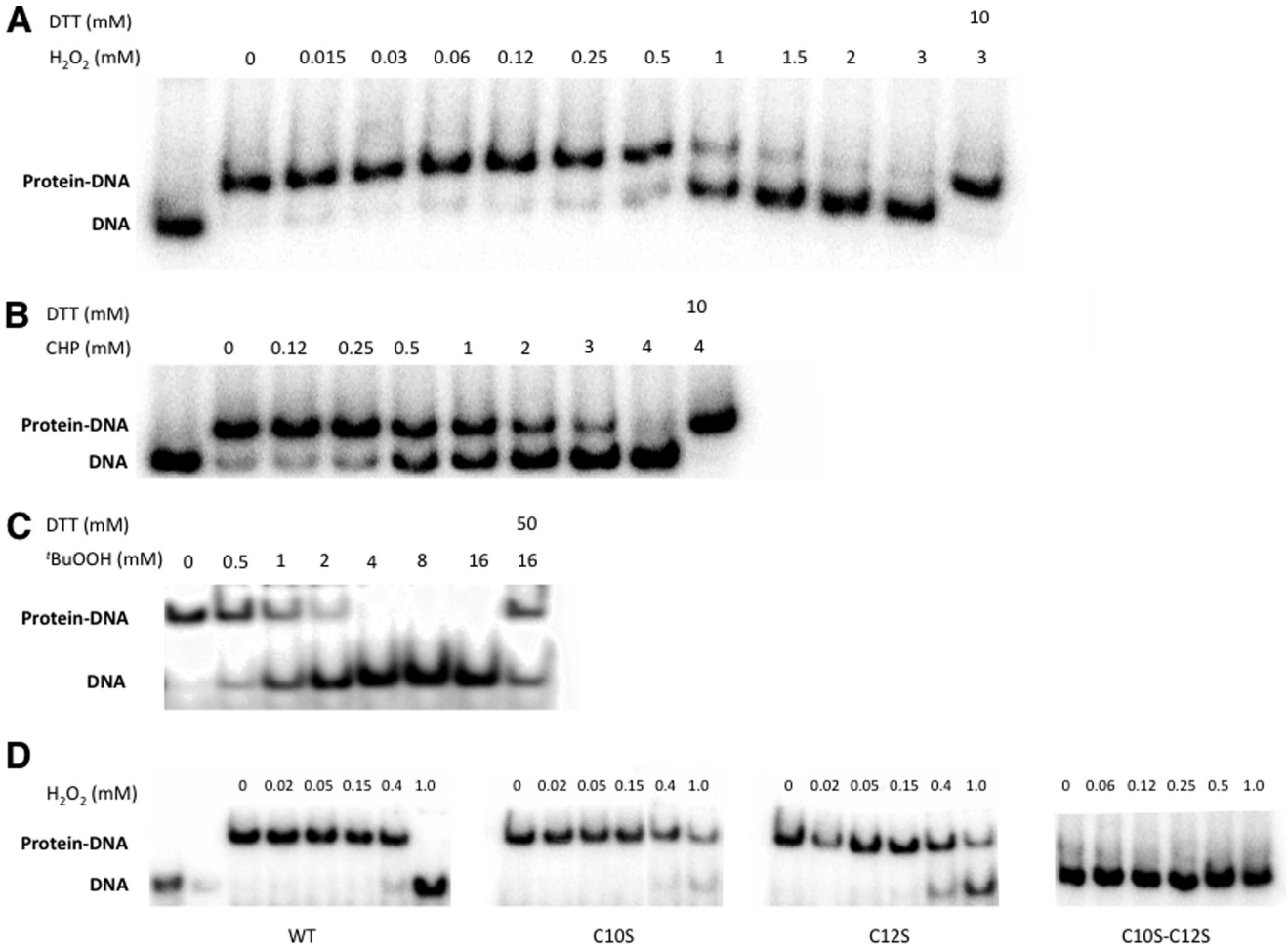

FIGURE 3. **MosR binds to DNA in an oxidation-dependent manner.** *A–C*, electrophoretic mobility shift assays of MosR (25 nM) with DNA (5 nM) upon increasing concentrations of oxidants: H_2O_2 (*A*); cumene hydroperoxide (*CHP*) (*B*); and *tert*-butyl hydroperoxide (^{t}*BuOOH*) (*C*). *D*, electrophoretic mobility shift assay for MosR, MosR_C10S, MosR_C12S, and MosR_C10SC12S upon increasing concentrations of H_2O_2. In this assay, complete dissociation is seen for the WT protein but not for the Cys-to-Ser substituted proteins. Double-substituted MosR_C10SC12S shows decreased DNA binding even under reducing conditions.

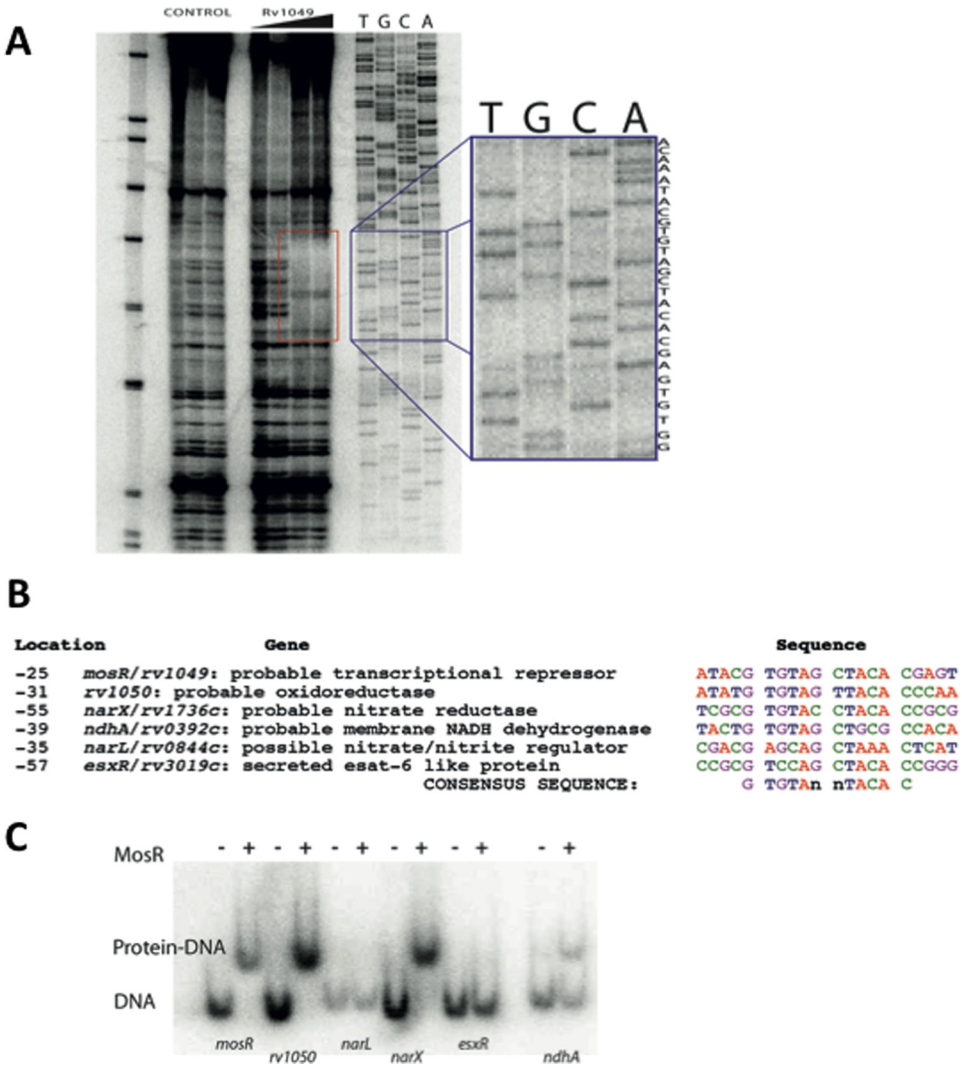

FIGURE 4. **MosR binds to a specific DNA sequence and controls expression of redox-related genes.** *A*, DNase I footprinting assay. The *red rectangle* indicates the region where the protein binds. The *blue rectangle* shows the sequence for that region: ACAA ATACG TGTAG | CTACA CGAGT CTGG. *B*, similar sequences are found in the promoter regions of *mosR*, *rv1050*, *narX*, *ndhA*, *narL*, and *esxR*. The *location number* indicates bases from the start codon. *C*, electrophoretic mobility shift assay showing that MosR binds to the promoter regions of *mosR*, *rv1050*, *narX*, and *ndhA*.

ing to those promoters and confirmed that in addition to binding to its own promoter, MosR can bind to the promoters of *rv1050* and *narX*, and to a lower extent, *ndhA* (Fig. 4*C*). These experiments allowed us to determine the sequence GTGTA*n* *n*TACAC (n = A, C, G, or T), as the consensus recognition motif of MosR. This motif is strictly conserved in the promoters of *mosR* (or *rv1049*), *rv1050*, and *narX* (or *rv1736c*), but it contains two mismatches in the promoters of *ndhA* and *esxR* and three in *narL* promoter, which explains why MosR does not bind to these promoters or why it does so with reduced affinity. Interestingly, Rv1050 and NarX are thought to be involved in reduction processes, which is consistent with being controlled by an oxidation-sensitive transcriptional regulator. Rv1050 is an exported protein (41) predicted to function as an oxidoreductase, and NarX is a predicted nitrite reductase, part of the *dosR* regulon, known to be induced by NO and hypoxia (42, 43).

MosR Structure Reveals a New Oxidation-sensing Mechanism—We next crystallized and solved the structures of MosR bound to a 28-bp duplex DNA and the apo form (Fig. 5, *A* and *B*). The MosR-DNA complex crystallized in the R3 space group, and the structure was solved to 3.1 Å resolution. Apo-MosR crystallized in the $P2_12_12_1$ space group and was solved to 2.7 Å resolution. In both structures, MosR forms a dimer of triangular shape with the two monomers related by noncrystallographic symmetry. These two structures resemble the structures of OhrR and SlyA with and without DNA (31, 44) (supplemental Fig. S4, *A* and *B*). Each monomer contains six α-helices and three antiparallel β-strands forming a β-sheet (there are only two β-strands in the DNA-bound structure as β1 becomes disordered). Strand β1 is longer than in related structures due to the insertion of five amino acids (Gly-51–Ile-55) between α2 and α3. Helices α1, α5, and α6 form the dimerization domain with α6 going over α1 helix of the adjacent monomer. Helices α3 and α4 and the connecting loop form the characteristic helix-turn-helix DNA-binding motif.

On the MosR-DNA complex structure, helices α1 and α1′ (prime refers to the opposing monomer) sit atop the DNA forming extensive contacts with the phosphate backbone on the minor groove of the DNA. α4 and α4′ fit into two consecutive major grooves recognizing the palindromic sequence

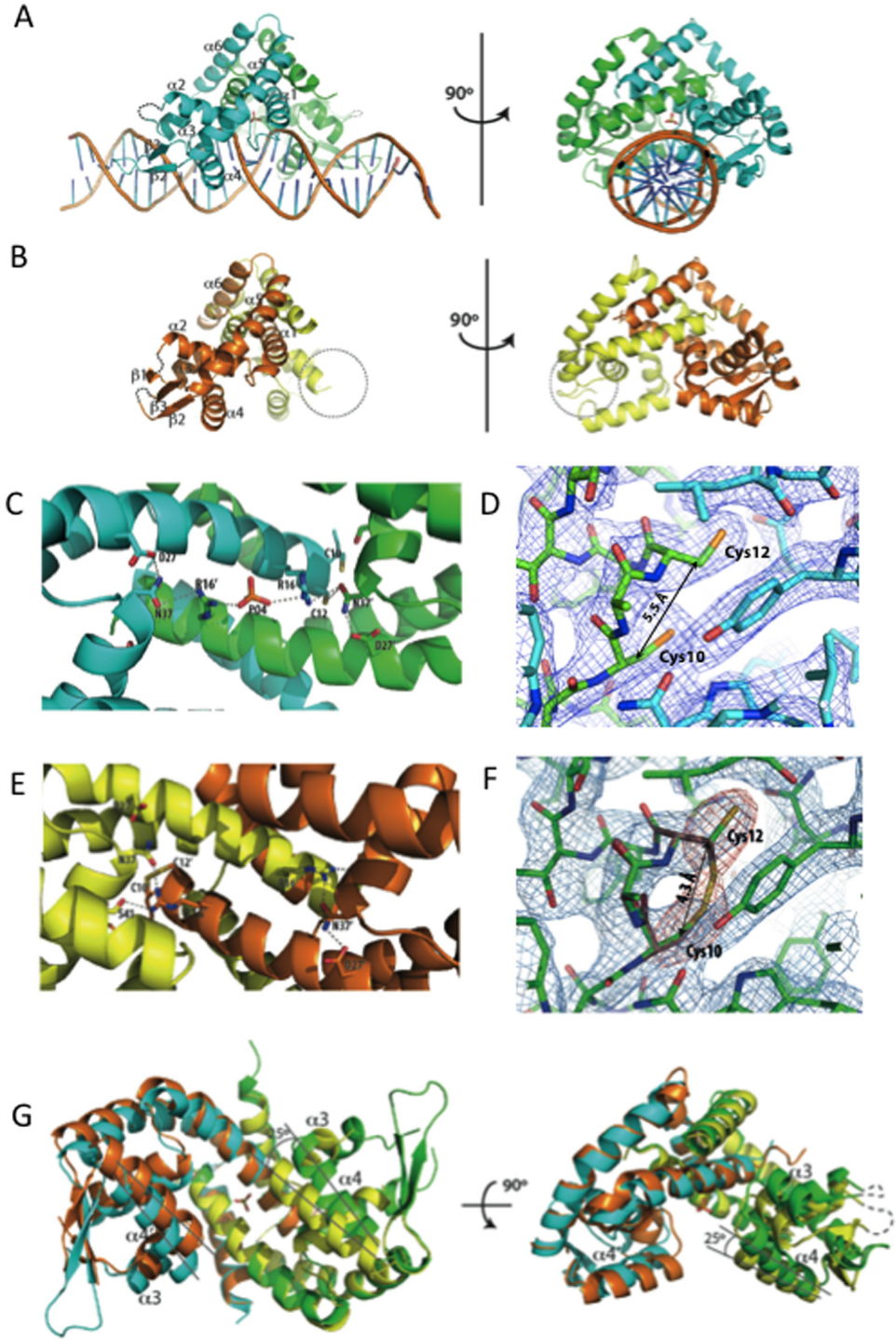

FIGURE 5. **The structure of MosR reveals oxidation-sensing mechanism.** *A*, reduced MosR-DNA structure. *B*, oxidized apo-MosR structure. The *dotted circle* indicates the wing region of chain B that had poor electron density and was not built. *C*, hydrogen-bonding interactions in the MosR-DNA (reduced) structure. *D*, detail of Cys-10–Cys-12 site in reduced MosR-DNA (reduced) structure. Electron density map corresponds to $2F_o$ - F_c map contoured at 1.5 σ. *E*, hydrogen-bonding interactions in the apo-MosR (oxidized) structure. *F*, detail of Cys-10–Cys-12 site in apo-MosR (oxidized) structure. In *red*, F_o - F_c simulated annealing omit maps for the sulfur atoms of Cys-10 and Cys-12 showing two possible conformations for Cys-12. *Blue maps* correspond $2F_o$ - F_c maps at 1.5 σ. *G*, superposition of the two structures seen from below and side (239 atoms, root mean square deviation = 1.83 Å^2). *Cyan* and *green*, MosR-DNA structure. *Orange* and *yellow*, apo-MosR. *Lines* indicate movement of α4.

GTGTAn nTACAC mainly through the side chains of Arg-70, Thr-71, Thr-72, and Asn-76 (supplemental Fig. S4, *C* and *D*). Between α4 and α5, there is a stretch of 21 amino acids forming two antiparallel β-strands (β2 and β3) that extend over the minor grooves making extensive contacts with phosphates, sugar oxygens, and the O_2 position of a thymidine base three bases away from the end of the palindrome. On the base of the triangle, the side chains of α1, α2, α1′, and α2′ form an extended array of hydrogen bonds parallel to the helices. Starting on one end, Cys-12 (α1) interacts with Asn-37′ (α2′) from

the other monomer, which further interacts with Arg-16 (α1) that is hydrogen-bonded to a phosphate ion situated in the center of the protein. Symmetrically, the phosphate interacts with Arg-16′ (α1′) from the other monomer, then Asn-37 (α2) and, finally, Cys-12′ (α1′) (Fig. 5*C*). In this structure, the C_β atoms of Cys-10 and Cys-12 are positioned 5.5 Å away from each other, and both thiol groups point toward the C terminus of the helix, representing clearly the reduced form of the protein (Fig. 5*D*).

The apo-MosR structure represents the oxidized conformation of the protein. The C_β atom of Cys-10 is positioned only 4.3 Å away from the C_β of Cys-12 (when compared with 5.5 Å in the reduced form), and Cys-12 can fit into the electron density in two alternate conformations, pointing up (or reduced) and pointing down forming disulfide (or oxidized) (Fig. 5*F*). Although there is electron density for the both the oxidized and the reduced conformations of Cys-12, the overall conformation of the protein is consistent with the oxidized state. The fact that the Cys-12 is partially reduced is indicative of the reversible nature of the disulfide bond, and we believe it to be due to the reducing power of electrons from the x-ray beam (45) because the overall conformation is very different from the reduced DNA-bound form.

From these structures, we can infer that when the disulfide bond is formed, there is rearrangement of hydrogen bonds and, consequently, a large change in the conformation of the protein. Inversion in the orientation of Cys-12 (α1) breaks the hydrogen bond to Asn-37′ (α2′) and brings Arg-16 (α1) closer, which forms a new hydrogen bond to Ser-41′ (α2′) (Fig. 5*E*). This new arrangement of hydrogen bonds results in the translation of α2 ~1.2 Å relative to α1. This movement in α2 pushes α3 ~4.5 Å toward α4, which then rotates ~25° inward to accommodate α3 (Fig. 5*G*). Rotation of α4 and α4′ prevents them from fitting into consecutive major grooves and thus impairs DNA binding.

With the structure at hand, we examined the possible roles of Cys-96 and Cys-147 in oxidation sensing. As mentioned above, by mass spectrometry, we found evidence of disulfide bond formation between these two cysteines. These cysteines are located on the surface of the protein and are more than 30 Å apart, which is incompatible with an intramolecular or interchain disulfide. This disulfide may arise from reaction between two dimers in solution. Formation of this second disulfide bond may be due to the strong oxidizing conditions employed experimentally, and it may or may not reflect a secondary oxidation-sensing mechanism of MosR that can be subjected to future studies.

Formation of an intramolecular disulfide bond between Cys-10 and Cys-12 is novel in this family of proteins. OhrR proteins can be classified as 1-Cys or 2-Cys proteins (46). 1-Cys proteins, typified by *B. subtilis* OhrR, have only one cysteine that can be oxidized to sulfenic acid or mixed disulfides (47), and this cysteine has been shown structurally in SarZ, another oxidation-sensitive transcriptional repressor from *S. aureus* (48). On the contrary, 2-Cys proteins, typified by *Xanthomonas campestris* OhrR, form intermolecular disulfide bond between the peroxidatic cysteine in the N terminus and a cysteine residue located on the C terminus of the other monomer (40, 49). To our knowledge, formation of a disulfide between two nearby cysteines from the same chain is unique to MosR and represents a new variant in oxidation sensing.

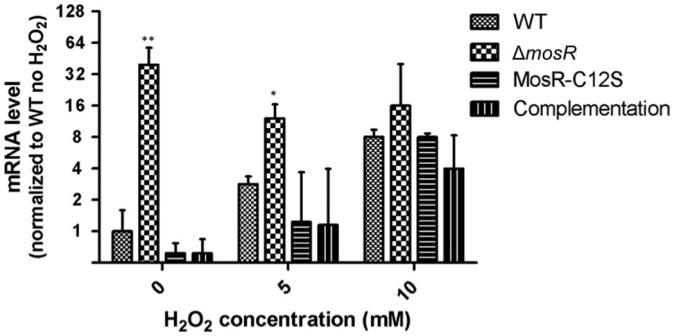

FIGURE 6. **MosR controls *rv1050* in response to oxidants.** RT-PCR analysis of *rv1050* expression in the wild-type, Δ*mosR*, MosR-C12S complementation, and MosR complementation strains during H_2O_2 treatment. Values are relative to wild-type strain under no H_2O_2 treatment. Results represent mean ± S.D. of three independent biological replicates and were normalized using *sigA* levels. (*, $p < 0.05$; **, $p < 0.01$ when compared with WT under the same treatment.).

MosR Deletion Was Generated by Double-crossover Homologous Recombination—Following the protocol by Parish and Stoker (36), we generated an unmarked in-frame deletion strain of *mosR* in *H37Rv* background (Δ*mosR*). This strain harbors a 441-bp deletion inside *mosR* (*rv1049*) gene corresponding to amino acids 2–148. This deletion was confirmed by PCR and Southern blotting (supplemental Fig. S5, *A* and *B*). We also generated a complementation strain (Δ*mosR*::pUC-*mosR* Hyg^R) by cloning *mosR* plus 318 bp upstream into the integrative plasmid pUC-GM-INT (50) and transforming Δ*mosR* cells with this plasmid. This strain was generated to ensure that any observed phenotypes were only due to the absence of *mosR* and not from inadvertent mutations introduced during cloning. We chose to include the promoter region to maintain similar expression levels as in wild-type strain. Additionally, this allowed us to perform site-directed mutagenesis in the complementation plasmid to generate a complementation strain expressing MosR-C12S to study the effect of this cysteine *in vivo*. Notably, mutation of *mosR* does not affect growth (supplemental Fig. S6), sensitivity to H_2O_2 and diamide, or sensitivity to the antituberculosis drugs isoniazid, rifampin, and ethambutol (supplemental Table S4).

Oxidation-responsive Transcriptional Regulation Was Confirmed in Vivo by RT-PCR—To verify that oxidation sensing is in fact occurring *in vivo*, we tested the mRNA levels of *rv1050* by RT-PCR using *sigA* as control. We extracted RNA of *M. tuberculosis* cultures grown to early log phase treated with 0, 5, and 10 mM H_2O_2 for 30 min. As shown in Fig. 6, without H_2O_2 treatment, the levels of *rv1050* mRNA on the Δ*rv1050* strain were 39-fold higher than in the wild-type strain, whereas the MosR and MosR-C12S complementation strains had levels similar to wild type (WT). Upon H_2O_2 treatment with 5 and 10 mM H_2O_2, the *rv1050* levels in WT went up by 5.6- and 27-fold, respectively, reaching levels comparable with Δ*mosR*. The Δ*mosR* strain had very high levels of rv1050 transcript in the absence of oxidants. The addition of H_2O_2 caused a slight decrease in the *rv1050* level, but it remained high when compared with uninduced WT. These results indicate that *rv1050* is fully up-regulated in the mutant and that MosR is the sole reg-

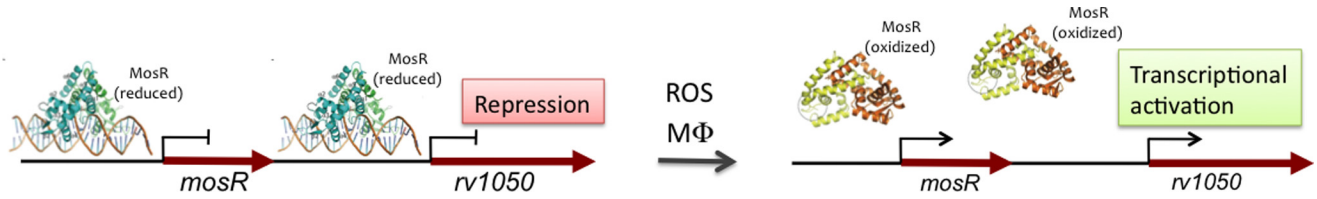

FIGURE 7. **Proposed model for MosR.** MosR is an oxidation-sensing transcriptional regulator of itself and *rv1050*. In the absence of oxidative stress, MosR binds to DNA, repressing transcription. Upon oxidative stress (as in the macrophage, Mø) MosR dissociates from DNA, enabling transcription of itself and *rv1050*.

ulator of *rv1050*. In the MosR-C12S complementation strain, there was a moderate 2.5-fold increase in *rv1050* message upon 5 mM treatment (when compared with 5.6-fold increase in WT, $p = 0.12$) and 30-fold increase upon 10 mM treatment (when compared with 27 in WT). This result shows that MosR-C12S is less sensitive to moderate concentrations of oxidants, which agrees with the trends observed by electromobility shift assays (Fig. 3). The complementary strain behaved similarly to WT strain in all the conditions. Similar trends were observed when probed by Northern blotting (supplemental Fig. S7).

The remarkably high levels of expression of *rv1050* upon H_2O_2 treatment suggest that this protein of unknown function plays an important role in adaptation to oxidative stress. Increase in *mosR* and *rv1050* expression upon the addition of oxidants has also been observed in previous microarray experiments with H_2O_2 (24) and diamide (51). Polyunsaturated fatty acids such as arachidonic acid and linoleic acid, which can readily undergo lipid peroxidation to generate ROS, also up-regulate the expression of *rv1050*, whereas saturated fatty acids such as oleic acid and palmitic acid down-regulate its expression.[3]

Global Gene Expression Profiling Shows Discrete Regulation by MosR—To determine the regulatory scope of MosR, we performed global gene expression profiling using RNA microarrays comparing the Δ*mosR* strain with *H37Rv* wild-type strain with and without H_2O_2 (supplemental Table S5). In the mutant *versus* WT under no H_2O_2 stress, we found only four genes that were differentially regulated: *rv0350*, *rv1050*, *rv1361c*, and *rv3478*. Out of these genes, *rv1050* showed the most significant difference (on average 352-fold higher in Δ*mosR* than wild type), whereas the other genes displayed modest induction (*rv0350*, *rv1361c*, and *rv2478*, range: −9.1- to 2.5-fold). Under 10 mM H_2O_2 treatment, there was no difference between the wild-type and Δ*mosR* strains in *rv1050* levels, which agrees with the RT-PCR results, and there were a total of nine genes, which showed 2–5-fold change (*fadA2*, *rpsS*, *rplP*, *rpsQ*, *rv0839*, *rv1884c*, *rv2558*, *rv3614c*, and *rv3615c*). None of these genes contain the consensus sequence in their promoter regions, and we attribute these changes to pleiotropic effects or to the perturbation of cellular pathways by the dramatic overexpression of *rv1050*.

Still, we were surprised not to find *narX* among the genes up-regulated in the Δ*mosR* strain. However, this can be explained by a second layer of regulation for this gene. It is known that *narX* is under the control of DosR and is only activated under hypoxia, nitric oxide, or carbon monoxide (43). It is possible that narX is under control of multiple regulators that need to work synergistically. In sum, this microarray experiment confirmed that MosR regulates *rv1050*, but unlike in *S. aureus*, where MgrA is a global regulator (17), *M. tuberculosis* MosR has narrow regulatory scope.

[3] Y. Liu and G. Schoolnik, TB Database.

DISCUSSION

In this study, we presented a new oxidation-sensing transcriptional repressor of *M. tuberculosis* that belongs to the MarR family, and its plausible mechanism (Fig. 7). We described the identification of MosR using a bioinformatics approach, the biochemical characterization of this protein showing that DNA binding is dependent on the oxidation state of the protein and that it is fully reversible. Based on x-ray crystallography and mass spectrometry, we proposed that oxidation sensing is facilitated by formation of a reversible disulfide bond between Cys-10 and Cys-12, a new mechanism among MarR proteins. We also identified the DNA-binding sequence for this regulator by DNase I footprinting and showed that similar sequences are present in the promoter regions of itself, *rv1050*, *narX*, and *ndhA*. To validate the function *in vivo*, we constructed a *mosR* deletion strain and demonstrated that MosR controls the expression of *rv1050* in response to oxidants using microarray and RT-PCR.

Interestingly, it had been shown previously that *rv1050* is up-regulated 2-fold during infection in INF-γ-activated macrophages (53). In light of our results, we can now explain that this up-regulation is likely due to MosR sensing ROS produced by the macrophage.

Another notable aspect about MosR comes from a study by Rengarajan *et al.* (54) that analyzed the genes required for survival in macrophages. This study found that a transposon insertion in *rv1049* (*mosR*) had the second largest increase in resistance to macrophage killing (5.6-fold increase). The authors note that the genes that give increased survival of the bacterium may pose a transcriptional burden under normal laboratory conditions. Now, based on our results, we can propose that mutation of *mosR* results in enhanced survival probably due to constitutively high expression of *rv1050*. Although we do not know the exact function of Rv1050, it likely has a protective effect in the bacterium. Unfortunately, that genome-wide study had no information on the effect of a transposon mutation directly on *rv1050* probably because the experiment was carried out using a heterogeneous culture (the TraSH library), and exported proteins such as Rv1050 could be produced by a neighboring bacterium masking its effect. It will be very interesting to test whether mutation of *rv1050* results in decreased intracellular survival.

Rv1050 is an exported protein predicted to function as an oxidoreductase. Given that arachidonic acid and linoleic acid are also among the signals that induce *rv1050* up-regulation, we

suspect that Rv1050 may affect fatty acid metabolism in the macrophage. It is known that *M. tuberculosis*-infected macrophages exhibit an altered arachidonic acid metabolism in favor of lipoxin A_4 over prostaglandin E_2 (PGE_2), which promotes necrosis over apoptosis (52, 55). Although it is unknown how *M. tuberculosis* affects this process, it is reasonable to conjecture that exported proteins are used to manipulate the metabolism of the macrophage. Furthermore, if Rv1050 is indeed important for the survival of *M. tuberculosis* in the macrophage, one could envision targeting this exported protein as a new avenue for therapy. Targeting exported proteins could be particularly interesting as it circumvents the challenge of the drugs getting into the bacterium.

Acknowledgments—We thank Prof. T. Parish for the mycobacterial plasmids, Prof. Linda Adams for helpful discussions, Dr. L. Zhang, Dr. C. B. Poor, and the beamline staff for help collecting the x-ray diffraction data, S. Alvarez and L. Hicks for assistance with the mass spectrometry experiments, H. Gutka and M. Rutter for assistance with M. tuberculosis cultures and media, and Dr A. Tevar for proofreading this manuscript. The use of the Advanced Photon Source (beamline 24-ID) at Argonne National Laboratory was supported by the United States Department of Energy.

REFERENCES

1. World Health Organization (2011) *Global Tuberculosis Control*, WHO Report 2011, pp. 1–27, World Health Organization, Geneva, Switzerland
2. Ehrt, S., and Schnappinger, D. (2009) Mycobacterial survival strategies in the phagosome: defense against host stresses. *Cell. Microbiol.* **11,** 1170–1178
3. Flynn, J. L., and Chan, J. (2001) Tuberculosis: latency and reactivation. *Infect. Immun.* **69,** 4195–4201
4. Buchmeier, N., and Fahey, R. C. (2006) The *mshA* gene encoding the glycosyltransferase of mycothiol biosynthesis is essential in *Mycobacterium tuberculosis* Erdman. *FEMS Microbiol. Lett.* **264,** 74–79
5. Buchmeier, N. A., Newton, G. L., and Fahey, R. C. (2006) A mycothiol synthase mutant of *Mycobacterium tuberculosis* has an altered thiol-disulfide content and limited tolerance to stress. *J. Bacteriol.* **188,** 6245–6252
6. Manca, C., Paul, S., Barry, C. E., 3rd, Freedman, V. H., and Kaplan, G. (1999) *Mycobacterium tuberculosis* catalase and peroxidase activities and resistance to oxidative killing in human monocytes *in vitro*. *Infect. Immun.* **67,** 74–79
7. Jackett, P. S., Aber, V. R., and Lowrie, D. B. (1978) Virulence and resistance to superoxide, low pH, and hydrogen peroxide among strains of *Mycobacterium tuberculosis*. *J. Gen. Microbiol.* **104,** 37–45
8. Piddington, D. L., Fang, F. C., Laessig, T., Cooper, A. M., Orme, I. M., and Buchmeier, N. A. (2001) Cu,Zn-superoxide dismutase of *Mycobacterium tuberculosis* contributes to survival in activated macrophages that are generating an oxidative burst. *Infect. Immun.* **69,** 4980–4987
9. Bryk, R., Griffin, P., and Nathan, C. (2000) Peroxynitrite reductase activity of bacterial peroxiredoxins. *Nature* **407,** 211–215
10. Bryk, R., Lima, C. D., Erdjument-Bromage, H., Tempst, P., and Nathan, C. (2002) Metabolic enzymes of mycobacteria linked to antioxidant defense by a thioredoxin-like protein. *Science* **295,** 1073–1077
11. Colangeli, R., Haq, A., Arcus, V. L., Summers, E., Magliozzo, R. S., McBride, A., Mitra, A. K., Radjainia, M., Khajo, A., Jacobs, W. R., Jr., Salgame, P., and Alland, D. (2009) The multifunctional histone-like protein Lsr2 protects mycobacteria against reactive oxygen intermediates. *Proc. Natl. Acad. Sci. U.S.A.* **106,** 4414–4418
12. McCann, J. R., McDonough, J. A., Sullivan, J. T., Feltcher, M. E., and Braunstein, M. (2011) Genome-wide identification of *Mycobacterium tuberculosis* exported proteins with roles in intracellular growth. *J. Bacteriol.* **193,** 854–861
13. Green, J., and Paget, M. S. (2004) Bacterial redox sensors. *Nat. Rev. Microbiol.* **2,** 954–966
14. den Hengst, C. D., and Buttner, M. J. (2008) Redox control in actinobacteria. *Biochim. Biophys. Acta* **1780,** 1201–1216
15. Chen, P. R., Brugarolas, P., and He, C. (2011) Redox signaling in human pathogens. *Antioxid. Redox Signal.* **14,** 1107–1118
16. Chen, P. R., Bae, T., Williams, W. A., Duguid, E. M., Rice, P. A., Schneewind, O., and He, C. (2006) An oxidation-sensing mechanism is used by the global regulator MgrA in *Staphylococcus aureus*. *Nat. Chem. Biol.* **2,** 591–595
17. Luong, T. T., Dunman, P. M., Murphy, E., Projan, S. J., and Lee, C. Y. (2006) Transcription profiling of the mgrA Regulon in *Staphylococcus aureus*. *J. Bacteriol.* **188,** 1899–1910
18. Luong, T. T., Newell, S. W., and Lee, C. Y. (2003) Mgr, a novel global regulator in *Staphylococcus aureus*. *J. Bacteriol.* **185,** 3703–3710
19. Ha, U., and Jin, S. (1999) Expression of the *soxR* gene of *Pseudomonas aeruginosa* is inducible during infection of burn wounds in mice and is required to cause efficient bacteremia. *Infect. Immun.* **67,** 5324–5331
20. Kobayashi, K., and Tagawa, S. (2004) Activation of SoxR-dependent transcription in *Pseudomonas aeruginosa*. *J. Biochem.* **136,** 607–615
21. Ochsner, U. A., Vasil, M. L., Alsabbagh, E., Parvatiyar, K., and Hassett, D. J. (2000) Role of the *Pseudomonas aeruginosa oxyR-recG* operon in oxidative stress defense and DNA repair: OxyR-dependent regulation of *katB-ankB*, *ahpB*, and *ahpC-ahpF*. *J. Bacteriol.* **182,** 4533–4544
22. Singh, A., Crossman, D. K., Mai, D., Guidry, L., Voskuil, M. I., Renfrow, M. B., and Steyn, A. J. (2009) *Mycobacterium tuberculosis* WhiB3 maintains redox homeostasis by regulating virulence lipid anabolism to modulate macrophage response. *PLoS Pathog.* **5,** e1000545
23. Singh, A., Guidry, L., Narasimhulu, K. V., Mai, D., Trombley, J., Redding, K. E., Giles, G. I., Lancaster, J. R., Jr., and Steyn, A. J. (2007) *Mycobacterium tuberculosis* WhiB3 responds to O_2 and nitric oxide via its [4Fe-4S] cluster and is essential for nutrient starvation survival. *Proc. Natl. Acad. Sci. U.S.A.* **104,** 11562–11567
24. Voskuil, M. I., Bartek, I. L., Visconti, K., and Schoolnik, G. K. (2011) The response of *Mycobacterium tuberculosis* to reactive oxygen and nitrogen species. *Front. Microbiol.* **2,** 105
25. Zahrt, T. C., Song, J., Siple, J., and Deretic, V. (2001) Mycobacterial FurA is a negative regulator of catalase-peroxidase gene *katG*. *Mol. Microbiol.* **39,** 1174–1185
26. Rodriguez, G. M., Voskuil, M. I., Gold, B., Schoolnik, G. K., and Smith, I. (2002) *ideR*, An essential gene in *Mycobacterium tuberculosis*: role of *IdeR* in iron-dependent gene expression, iron metabolism, and oxidative stress response. *Infect. Immun.* **70,** 3371–3381
27. Fernandes, N. D., Wu, Q. L., Kong, D., Puyang, X., Garg, S., and Husson, R. N. (1999) A mycobacterial extracytoplasmic sigma factor involved in survival following heat shock and oxidative stress. *J. Bacteriol.* **181,** 4266–4274
28. Wu, Q. L., Kong, D., Lam, K., and Husson, R. N. (1997) A mycobacterial extracytoplasmic function sigma factor involved in survival following stress. *J. Bacteriol.* **179,** 2922–2929
29. Otwinowski, Z., and Minor, W. (1997) Processing of X-ray diffraction data collected in oscillation mode *Methods Enzymol.* **276,** 307–326
30. McCoy, A. J., Grosse-Kunstleve, R. W., Adams, P. D., Winn, M. D., Storoni, L. C., and Read, R. J. (2007) Phaser crystallographic software. *J. Appl. Crystallogr.* **40,** 658–674
31. Hong, M., Fuangthong, M., Helmann, J. D., and Brennan, R. G. (2005) Structure of an OhrR-*ohrA* operator complex reveals the DNA binding mechanism of the MarR family. *Mol. cell* **20,** 131–141
32. Adams, P. D., Afonine, P. V., Bunkóczi, G., Chen, V. B., Davis, I. W., Echols, N., Headd, J. J., Hung, L. W., Kapral, G. J., Grosse-Kunstleve, R. W., McCoy, A. J., Moriarty, N. W., Oeffner, R., Read, R. J., Richardson, D. C., Richardson, J. S., Terwilliger, T. C., and Zwart, P. H. (2010) PHENIX: a comprehensive Python-based system for macromolecular structure solution. *Acta Crystallogr. D Biol. Crystallogr.* **66,** 213–221
33. Emsley, P., Lohkamp, B., Scott, W. G., and Cowtan, K. (2010) Features and development of Coot. *Acta Crystallogr. D Biol. Crystallogr.* **66,** 486–501
34. DeLano, W. L. (2010) *The PyMOL Molecular Graphics System*, version 1.3r1, Schrödinger, LLC, New York

35. Leblanc, B., and Moss, T. (1994) DNase I footprinting. *Methods Mol. Biol.* **30,** 1–10
36. Parish, T., and Stoker, N. G. (2000) Use of a flexible cassette method to generate a double unmarked *Mycobacterium tuberculosis tlyA plcABC* mutant by gene replacement. *Microbiology* **146,** 1969–1975
37. Wilson, M., Voskuil, M., Schnappinger, D., and Schoolnik, G. K. (2001) Functional genomics of *Mycobacterium tuberculosis* using DNA microarrays. *Methods Mol. Med.* **54,** 335–357
38. Ta, P., Buchmeier, N., Newton, G. L., Rawat, M., and Fahey, R. C. (2011) Organic hydroperoxide resistance protein and ergothioneine compensate for loss of mycothiol in *Mycobacterium smegmatis* mutants. *J. Bacteriol.* **193,** 1981–1990
39. Poole, L. B., and Nelson, K. J. (2008) Discovering mechanisms of signaling-mediated cysteine oxidation. *Curr. Opin. Chem. Biol.* **12,** 18–24
40. Panmanee, W., Vattanaviboon, P., Poole, L. B., and Mongkolsuk, S. (2006) Novel organic hydroperoxide-sensing and responding mechanisms for OhrR, a major bacterial sensor and regulator of organic hydroperoxide stress. *J. Bacteriol.* **188,** 1389–1395
41. Målen, H., Berven, F. S., Fladmark, K. E., and Wiker, H. G. (2007) Comprehensive analysis of exported proteins from *Mycobacterium tuberculosis* H37Rv. *Proteomics* **7,** 1702–1718
42. Sherman, D. R., Voskuil, M., Schnappinger, D., Liao, R., Harrell, M. I., and Schoolnik, G. K. (2001) Regulation of the *Mycobacterium tuberculosis* hypoxic response gene encoding α-crystallin. *Proc. Natl. Acad. Sci. U.S.A.* **98,** 7534–7539
43. Voskuil, M. I., Schnappinger, D., Visconti, K. C., Harrell, M. I., Dolganov, G. M., Sherman, D. R., and Schoolnik, G. K. (2003) Inhibition of respiration by nitric oxide induces a *Mycobacterium tuberculosis* dormancy program. *J. Exp. Med.* **198,** 705–713
44. Dolan, K. T., Duguid, E. M., and He, C. (2011) Crystal structures of SlyA protein, a master virulence regulator of Salmonella, in free and DNA-bound states. *J. Biol. Chem.* **286,** 22178–22185
45. Petrova, T., Ginell, S., Mitschler, A., Kim, Y., Lunin, V. Y., Joachimiak, G., Cousido-Siah, A., Hazemann, I., Podjarny, A., Lazarski, K., and Joachimiak, A. (2010) X-ray-induced deterioration of disulfide bridges at atomic resolution. *Acta Crystallogr. D Biol. Crystallogr.* **66,** 1075–1091
46. Antelmann, H., and Helmann, J. D. (2011) Thiol-based redox switches and gene regulation. *Antioxid. Redox Signal* **14,** 1049–1063
47. Lee, J. W., Soonsanga, S., and Helmann, J. D. (2007) A complex thiolate switch regulates the Bacillus subtilis organic peroxide sensor OhrR. *Proc. Natl. Acad. Sci. U.S.A.* **104,** 8743–8748
48. Poor, C. B., Chen, P. R., Duguid, E., Rice, P. A., and He, C. (2009) Crystal structures of the reduced, sulfenic acid, and mixed disulfide forms of SarZ, a redox active global regulator in *Staphylococcus aureus*. *J. Biol. Chem.* **284,** 23517–23524
49. Newberry, K. J., Fuangthong, M., Panmanee, W., Mongkolsuk, S., and Brennan, R. G. (2007) Structural mechanism of organic hydroperoxide induction of the transcription regulator OhrR. *Mol. Cell* **28,** 652–664
50. Mahenthiralingam, E., Marklund, B. I., Brooks, L. A., Smith, D. A., Bancroft, G. J., and Stokes, R. W. (1998) Site-directed mutagenesis of the 19-kilodalton lipoprotein antigen reveals no essential role for the protein in the growth and virulence of *Mycobacterium intracellulare*. *Infect Immun.* **66,** 3626–3634
51. Fontán, P. A., Voskuil, M. I., Gomez, M., Tan, D., Pardini, M., Manganelli, R., Fattorini, L., Schoolnik, G. K., and Smith, I. (2009) The *Mycobacterium tuberculosis* sigma factor σ^B is required for full response to cell envelope stress and hypoxia *in vitro*, but it is dispensable for *in vivo* growth. *J. Bacteriol.* **191,** 5628–5633
52. Divangahi, M., Desjardins, D., Nunes-Alves, C., Remold, H. G., and Behar, S. M. (2010) Eicosanoid pathways regulate adaptive immunity to *Mycobacterium tuberculosis*. *Nat. Immunol.* **11,** 751–758
53. Schnappinger, D., Ehrt, S., Voskuil, M. I., Liu, Y., Mangan, J. A., Monahan, I. M., Dolganov, G., Efron, B., Butcher, P. D., Nathan, C., and Schoolnik, G. K. (2003) Transcriptional adaptation of *Mycobacterium tuberculosis* within macrophages: insights into the phagosomal environment. *J. Exp. Med.* **198,** 693–704
54. Rengarajan, J., Bloom, B. R., and Rubin, E. J. (2005) Genome-wide requirements for *Mycobacterium tuberculosis* adaptation and survival in macrophages. *Proc. Natl. Acad. Sci. U.S.A.* **102,** 8327–8332
55. Chen, M., Divangahi, M., Gan, H., Shin, D. S., Hong, S., Lee, D. M., Serhan, C. N., Behar, S. M., and Remold, H. G. (2008) Lipid mediators in innate immunity against tuberculosis: opposing roles of PGE_2 and LXA_4 in the induction of macrophage death. *J. Exp. Med.* **205,** 2791–2801